

D5.5



SPECIFICATIONS FOR BEACON WP5: TESTING, VERIFICATION AND VALIDATION OF MODELS STEP 3

DELIVERABLE D5.5 Report

Author(s): **María Victoria Villar, Jean Talandier**

Reporting period: 01/12/18 – 31/05/20

Date of issue of this report: **xx/xx/2020**

Start date of project: **01/06/17**

Duration: 48 Months

This project receives funding from the Euratom research and training programme 2014-2018 under grant agreement No 745 942		
Dissemination Level		
PU	Public	X

REVIEW

Name	Internal/Project/External	Comments

DISTRIBUTION LIST

Name	Comments
Renata Bachorczyk-Nagy (EC) Christophe Davies (EC) Beacon partners	

Abstract

One of the main challenges in modelling swelling materials is the capacity of the models to perform predictive simulations. The presence of initial heterogeneities in these materials or heterogeneities due to external conditions increases the complexity of predicting the evolution of swelling clay materials. The idea is to select some tests performed in WP4 from BEACON project.

CIEMAT has planned to carry out a series of tests in an oedometer with two layers: one made with pellets mixture, the other made with a compacted block. This situation implies an initial heterogeneity in the material and the evolution of this heterogeneity is followed during the test.

Three tests are proposed for this exercise: two tests already completed to offer the partners the possibility to calibrate their models, one test where only the initial and boundary conditions are given. On this last test, a blind prediction is expected from the participants.

Content

1	Introduction	5
2	Description of the tests	5
2.1	Equipment.....	5
2.2	Preparation of specimens.....	7
2.3	Test procedure	8
2.4	Parameters.....	8
2.5	Results for test MGR22 and MGR23	8
2.6	Results for test MGR27	14
2.7	Requested outputs.....	14
	References	16

1 Introduction

CIEMAT carried out a series of hydration tests in isochoric cells to evaluate the evolution of bentonite during hydration, initially put in place in a heterogeneous way (Table 1-1). The half of the cell is filled with bentonite pellets with an average dry density close to 1.30 g/cm³ and the other part with a bentonite block with a dry density of 1.60 g/cm³. Hydration with deionised water takes place through the bottom.

Table 1-1 *List of constant volume tests performed by CIEMAT*

Test	Hydration	Duration (days)	T (°C)
MGR21	Constant pressure: 15 kPa	34	23.1±0.6
MGR22	Constant flow: 0.05 cm ³ /h	266	22.4±1.3
MGR23	Constant pressure: 15 kPa	210	22.6±1.5
MGR24	Constant pressure: 15 kPa	14	22.5±0.6
MGR25	Constant pressure: 15 kPa	76	22.7±1.1
MGR26	Constant flow: 0.05 cm ³ /h	132	23.6±1.2
MGR27	Constant pressure: 15 kPa	-	

Among a set of seven experiments, two of them have been selected to compare the experimental results with the models (MGR22 and MGR23). The main interest is that the tests are performed with the same conditions except the boundary conditions concerning the water supply. In one case, a constant pressure is imposed (MGR23) and in the other a constant flow is imposed (MGR22). In these two tests, pellets layer is placed in the lower part of the cell and the block in the upper part.

One test has been selected for predictive modelling (MGR27). The conditions of the test are similar to test MGR23 except that the pellets layer is located in the upper part of the cell and block on the lower part.

2 Description of the tests

2.1 Equipment

Tests have been performed at constant volume in oedometer. It consists of a cylindrical body with base and an upper piston that may move in the cylinder (Figure 2-1, Figure 2-2). The body has an inner diameter of 10 cm and the length of the sample inside was 10 cm. The top and bottom of the sample were in contact with filter papers and ceramic porous discs connected to outlets. The cell was placed in a rigid frame that guaranteed the constant volume of the sample by hindering the displacement of the piston. An external LVDT measured the potential axial displacements, whereas a 10-t load cell in the upper part of the frame

measured the force developed by the specimen.
Water is supplied through the bottom of the sample via a porous disc.

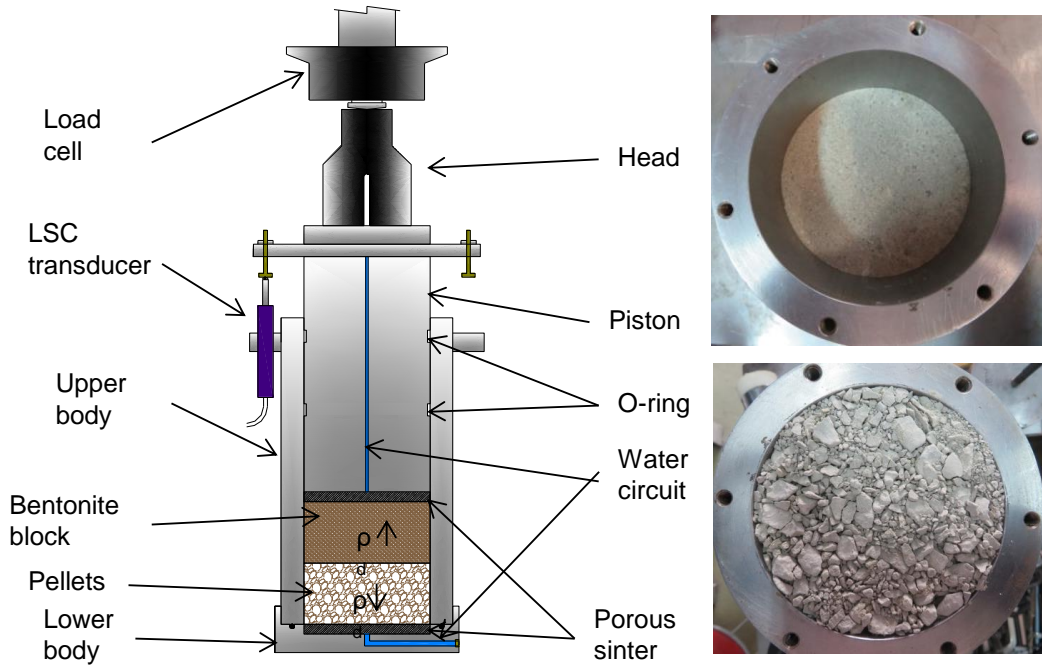


Figure 2-1 Schematic representation of the MGR cell – MGR22 and MGR23 (left) and images of the block (upper right) and pellets (lower right)

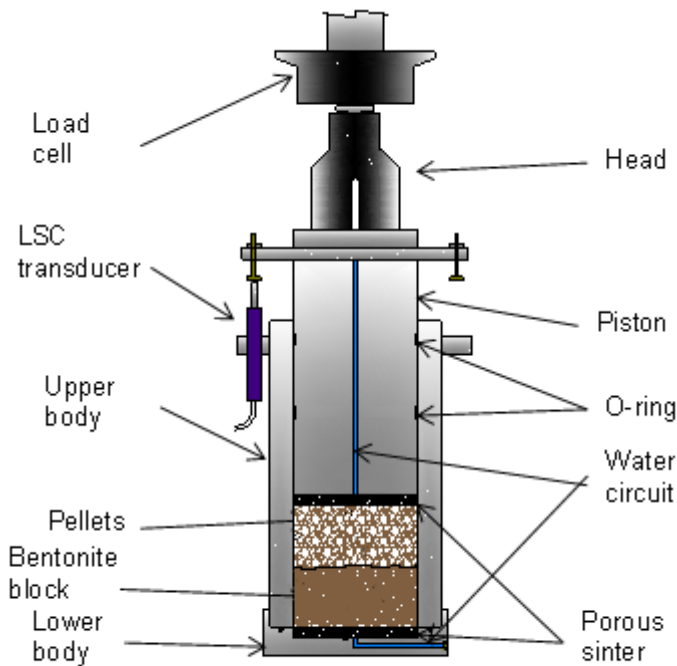


Figure 2-2 Schematic representation of the MGR27 cell

2.3 Preparation of specimens

The material used in all the tests was the FEBEX bentonite. The block part of the sample was compacted from the granulate material with its hygroscopic water content, which is ~14%. The pellets were prepared in a factory for the EB project (ENRESA 2005). The bentonite was dried and milled in a three-step process to produce a fine grade powder with a water content of 3.3%. Later, a commercial plant with an in-line highly automated briquetting process produced coarse (>7 mm) and fine (0.4-2 mm) grained materials with dry densities of 2.11 and 2.13 g/cm³, respectively. These two grain size fractions were subsequently combined to fit a Fuller shape curve with a maximum diameter of 12.7 mm and a minimum diameter of 0.425 mm, in order to reduce segregation. The different grain sizes were kept separated and mixed in the right proportion just before every test. The lab ran out of pellets larger than 9.5 mm, and the granulometric distribution of tests MGR23 and MGR27 was modified to keep the Fuller's curve (Table 2-1). Also, in these tests the pellets were softly dried to a water content closer to the fabrication one, because the water content of the pellets increased during storage.

Table 2-1 Granulometric curve of the pellets of Febex bentonite used in the tests

Sieve sizes (mm)	Percentage retained (%)	
	MGR22	MGR23/MGR27
9.5	17	0
4.75	31	37
2.0	26	31
1.18	11	13
0.59	10	12
0.425	5	6

The bentonite block was directly compacted inside the cell and the pellets were poured on it and carefully shaken as necessary to get the target density. Depending of the case, the cell was overturned (MGR22, 23) or not (MGR27). Initial characteristics of the two layers are given in Table 2-2 for tests MGR22 and MGR23.

Table 2-2 Initial characteristics of MGR22 and MGR23 tests

	w (%)	h (cm)	ρ_d (g/cm ³)	S_r (%)	w (%)	h (cm)	ρ_d (g/cm ³)	S_r (%)
Test	MGR22				MGR23			
Pellets	9.9	5.04	1.28	25	3.5	5.00	1.30	9
Block	13.6	4.94	1.61	55	14.2	4.98	1.60	56
Total	11.9	9.98	1.45	37	9.4	9.98	1.45	29

Initial characteristics of the two layers are given in Table 2-2 for tests MGR27.

Table 2-3 Initial characteristics of MGR27 tests

	w (%)	h (cm)	ρ_d (g/cm ³)	S_r (%)
Test	MGR27			
Pellets	3.5	5.00	1.30	9
Block	14.2	4.98	1.60	56
Total ^b	9.4	9.98	1.45	29

2.4 Test procedure

The water intake took place through the bottom surface. For MGR22 test, a low constant flow is imposed simulating a continuous contribution of water representative of e.g. Grimsel granite conditions. For MGR23 test, a constant pressure is imposed simulating reduced water intake conditions representative of e.g. Opalinus clay in Mont Terri (see Table 2-4). Deionised water was used in both cases.

Table 2-4 Conditions of hydration for each test

Test	Hydration	T (°C)
MGR22	Constant flow: 0.05 cm ³ /h	22.4±1.3
MGR23	Constant pressure: 14 kPa	22.6±1.5
MGR27	Constant pressure: 14 kPa	

In the first case (MGR22), the water intake was measured with a pressure/volume controlled and in other cases (MGR23, MGR27) with an automatic volume change apparatus. During hydration the top outlet remained open to atmosphere and the pressure exerted by the material, the sample deformation and the water intake were measured and automatically recorded. The tests were performed at laboratory temperature.

At the end of the tests, the bentonite block was extracted from the cell and it was subsampled to determine water content, dry density and pore size distribution at different levels along the height. The blocks from MGR tests were sliced in 6 horizontal levels (3 for pellets and 3 for block).

2.5 Parameters

All parameters for this material can be found in D5.2.1 report from task 5.2 and in Hoffman et al, 2007.

2.6 Results for test MGR22 and MGR23

Two types of online results are available for the two tests: the water intake by the sample as a function of time and the swelling pressure measured on the top of the sample.

Figure 2-3 shows the evolution of water intake and axial pressure for the two MGR

tests.

A significantly different behaviour is observed between the test performed under constant injection pressure MGR23 and the test MGR22 performed under constant water inflow rate.

In the test MGR23, the water intake was very quick and more than half of the water volume necessary for full saturation was taken in about 10 days.

In the test MGR22, when full saturation was reached, the injection pressure started to increase (the equipment was not able to keep a constant low injection flow into a saturated sample without increasing the injection pressure), and this explains the odd final shape of the curves.

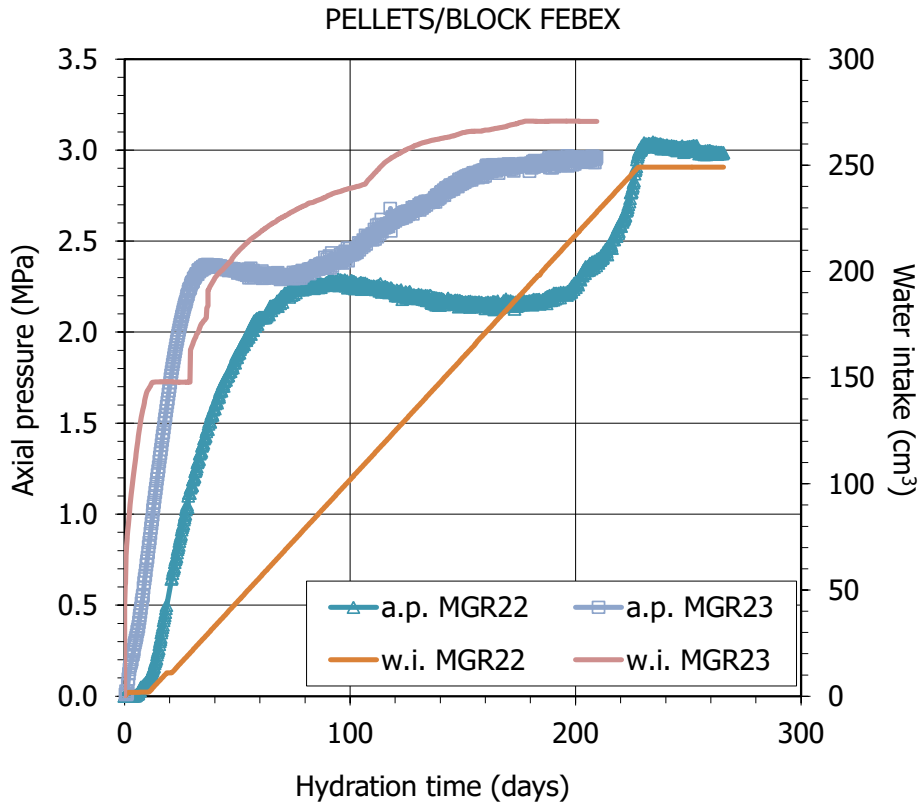


Figure 2-3 Water intake and axial pressure evolution in MGR tests (constant flow was prescribed in test MGR22)

Figure 2-4 shows the evolution of axial pressure in function of water intake in both cases and highlights the influence of the boundary condition on the swelling processes.

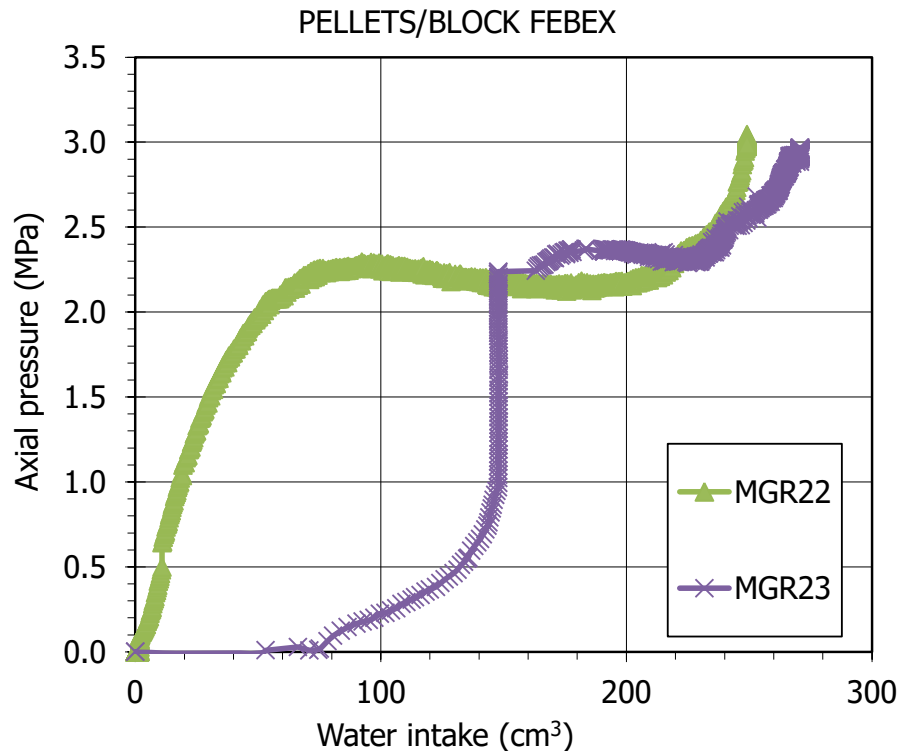


Figure 2-4 Axial pressure function of water intake for MGR22 and MGR23 tests

For the two tests, the swelling pressure expected for a FEBEX bentonite sample compacted to the average dry density value of the MGR tests (1.45 g/cm^3) is exceeded ($\sim 3 \text{ MPa}$). The theoretical value would be $2.0 \pm 0.5 \text{ MPa}$, according to the empirical correlation between dry density and swelling pressure obtained in small standard oedometers (Villar 2002, Villar & Lloret 2008). Previous researches showed that there is a scale effect on the swelling pressure measured in the laboratory, which tends to be higher as the testing cell is larger (Imbert & Villar 2006). This could maybe explain the higher pressure obtained in the large-scale oedometer with respect to the theoretical value obtained from empirical correlations.

The final appearance of the samples once extracted from the cell is shown in Figure 2-5. The upper part (block) and the lower one (pellets) are sealed at the end of the test and can only be separated with a knife.



MGR23: 210 days MGR22: 266 days

Figure 2-5 *Appearance of the MGR samples at the end of the tests*

The water content and dry density measured in subsamples after dismantling are plotted in Figure 2-6 and Figure 2-7 as a function of the distance to the hydration surface (i.e. the cell bottom). The initial values are indicated with thick horizontal lines. In test MGR23 the pellets were dried to the values they had after manufacturing. During the tests the water content and degree of saturation increased overall, although it decreased from the hydration surface (sample bottom) upwards whereas the dry density increased in this sense. These gradients were steeper as the test duration was shorter and attenuated over time (not shown in these figures). The pellets/block interface did not seem to have any effect on the continuous gradients. The final dry density and water content values were similar in the two longest tests (MGR22, MGR23), despite the different hydration conditions (constant flow or pressure). Although the bentonite was finally fully saturated, the dry density and water content along the samples is not uniform at the end.

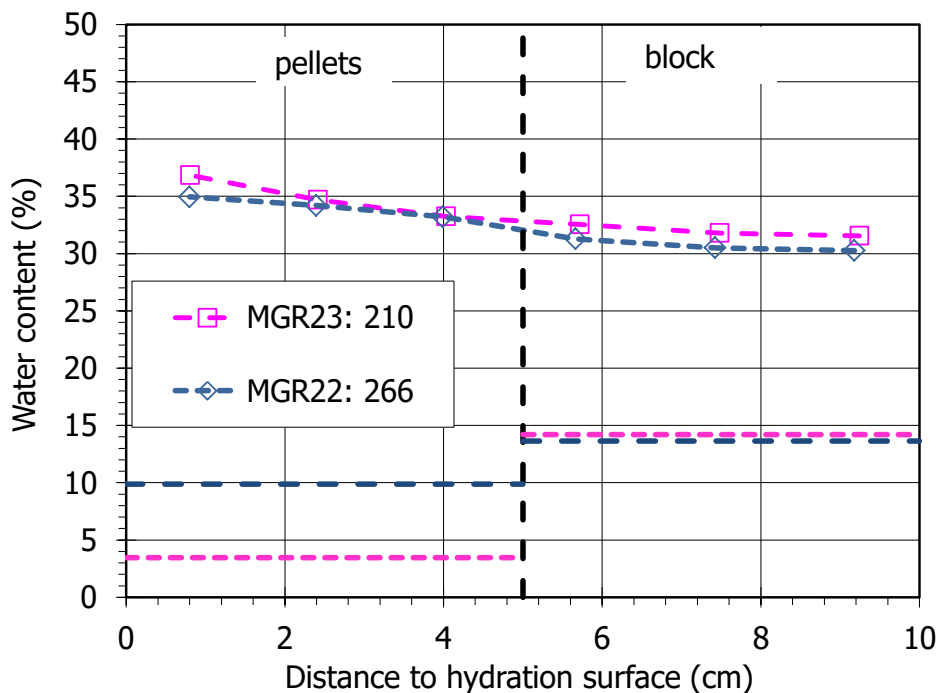


Figure 2-6 *Final water content along the samples of MGR tests. The duration of the tests is indicated in days. The thick horizontal lines indicate the initial values*

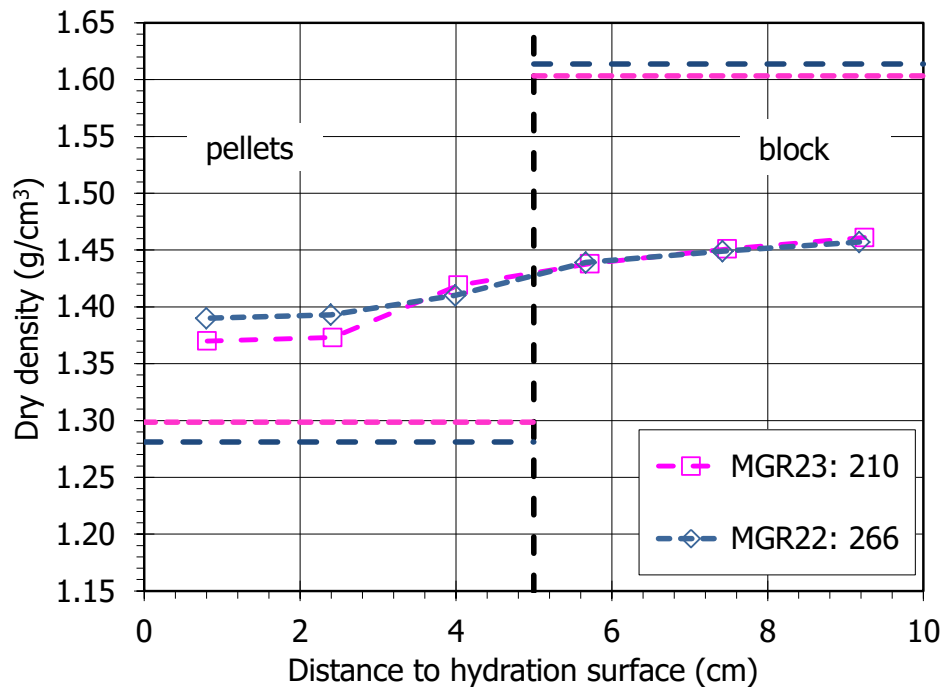


Figure 2-7 Final dry density along the samples of MGR tests. The duration of the tests is indicated in days. The thick horizontal lines indicate the initial values

Final characteristics of the samples are given in Table 2-5.

Table 2-5 Final characteristics of MGR tests

	w (%)	h (cm)	ρ_d (g/cm ³)	S_r (%)	w (%)	h (cm)	ρ_d (g/cm ³)	S_r (%)
Test	MGR22				MGR23			
Pellets	35.3	1.35	4.79	95	35.7	1.34	4.84	95
Block	30.7	1.51	5.27	106	31.1	1.51	5.29	107
Total ^a	33.9	1.44	10.01	105	33.2	1.45	10.01	103
Total ^b	32.7	1.43	10.06	100	33.2	1.43	10.12	101

^a from online measurements, in test MGR22 the water intake includes the intake of the porous stone, ^b from measurement of dimensions and water content, the final values affected by decompression

Analysis of the final pore size distribution has been done at several locations (3 in the block part and 3 in the initial pellets part). As an example, Figure 2-8 shows the incremental curves of mercury intrusion for MGR23 samples and for FEBEX samples of the same characteristics as the initial conditions used in the cells. For the block part of the samples, the curve corresponding to a sample compacted at dry density 1.59 g/cm³ with a water content of 14% was used. For the pellets part, a mixture of pellets having approximately a Fuller's curve grain size distribution, with a resulting dry density of 1.29 g/cm³ and a water content of 10%, was used. The usual two pore families corresponding approximately to pores larger and smaller than 200 nm could be told apart in all samples, except for the initial pellets curve, which showed that

most of the pores had a size around 300 μm .

The pore size distribution of the pellet half significantly changed. Although most of the porosity still corresponded to pores larger than 200 nm, the size of these pores decreased with respect to the initial pellets mixture, particularly for the subsamples taken farther away from the hydration surface. In the subsamples from the block half, the size of the macropores increased with respect to the original block, whereas in the pellets half, the percentage of pores smaller than 200 nm increased and the size of the macropores decreased with respect to the original pellets.

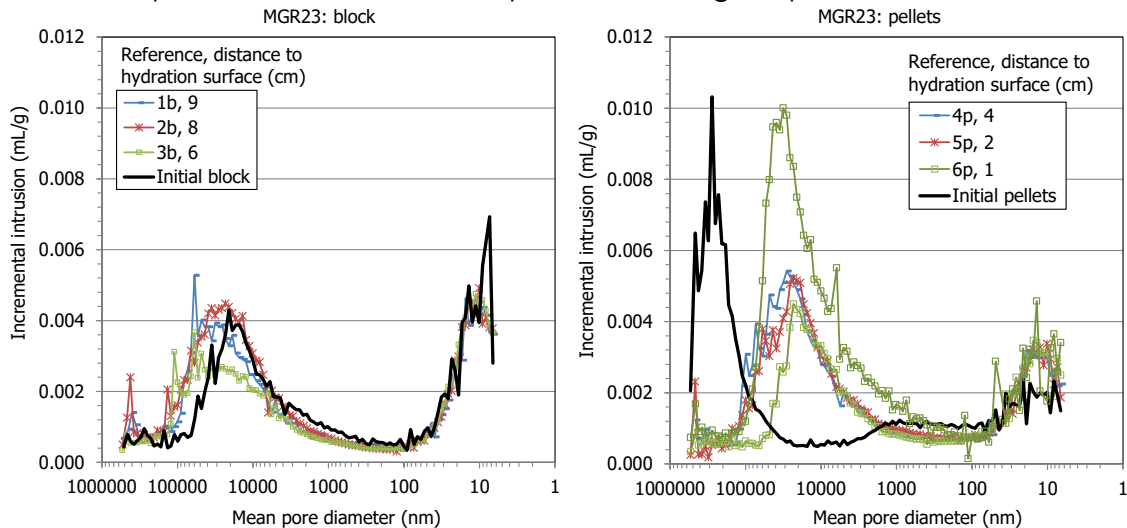


Figure 2-8 Pore size distribution expressed as incremental mercury intrusion of samples from the MGR23 test (lasting 210 days), corresponding to the block (left) and pellets (right) halves. In both cases the curves for the initial materials (blocks and pellets) are included

The percentage of pores intruded by mercury in these subsamples was between 35 and 70%. Taking this into account, the void ratio corresponding to pores larger and smaller than 200 nm was recalculated. In all cases the largest proportion of void ratio corresponded to the pores of diameter smaller than 200 nm, but the relationship between the void ratio corresponding to pores smaller (e_m) and larger (e_M) than 200 nm increased in all tests, which would indicate an increase in the volume of macropores during testing (Figure 2-9).

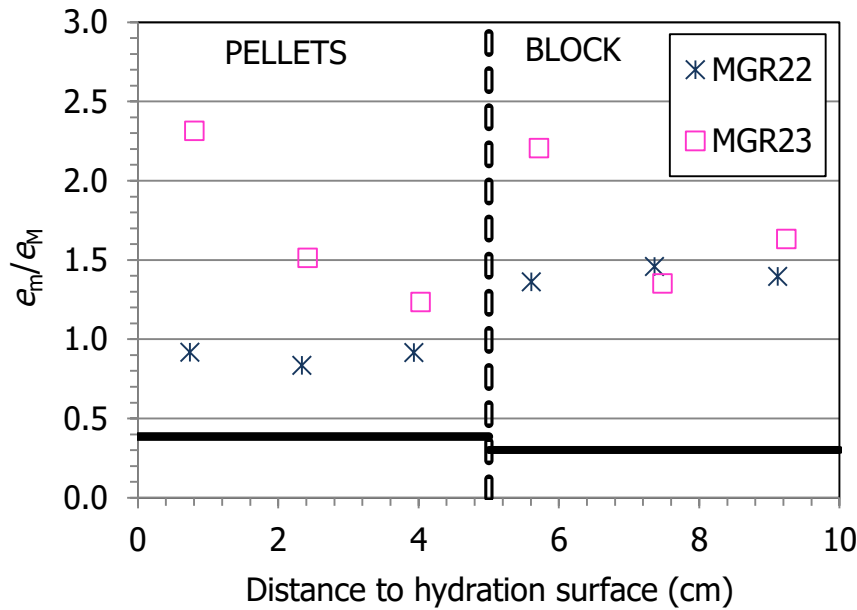


Figure 2-9 Ratio between void ratio corresponding to pores smaller and larger than 200 nm (e_m and e_M) obtained by MIP in subsamples from the MGR tests (the thick horizontal lines indicate the initial conditions)

2.7 Results for test MGR27

No results are given at this stage for this test. It is expected some blind predictions of the behavior.

2.8 Requested outputs

Two level of information should be given:

- Brief description of the model and the parameter used. How the model is calibrated for this specific test.
- Results from the test at several locations and for a predefined list of time. To facilitate the comparison of results, an Excel form will be provided to be filled by the participants.

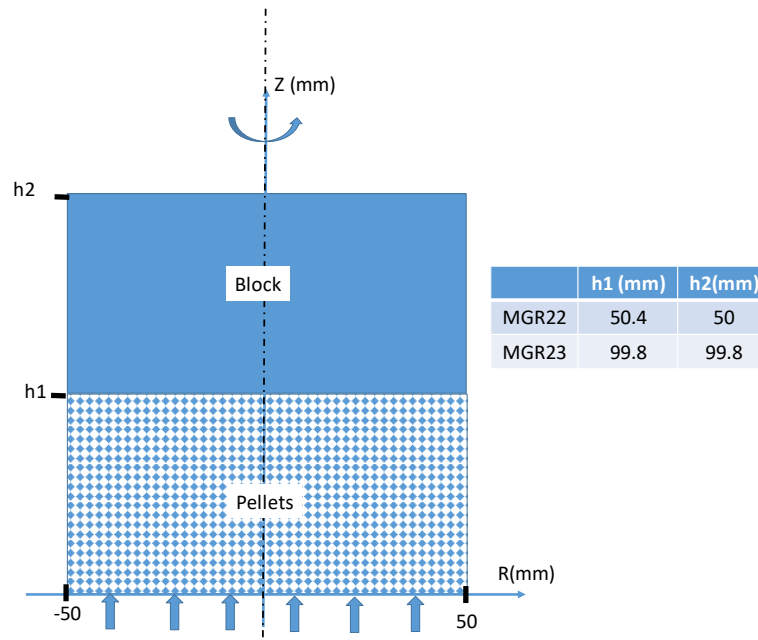


Figure 2-10 Schematic 2D-representation of the set up for MGR22 and MGR23

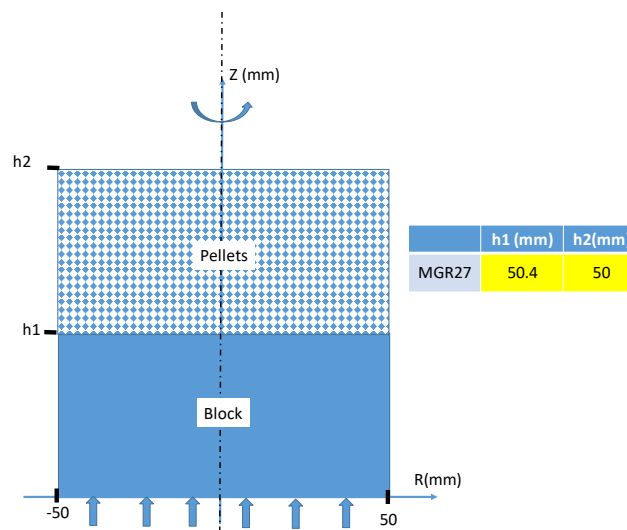


Figure 2-11 Schematic 2D-representation of the set up for MGR27

The requested outputs from the two tests are:

- Total axial stress function of time on the top and **on the bottom** of the cell at $z=0$ and $z=100\text{mm}$
- Total radial stress function of time at $z=25$, $z=75$ mm on cell wall
- Dry density and water content function of time at ($R=0\text{mm}$, $z=12, 30, 50, 67, 95\text{mm}$)
- Dry density and water content profiles at $z=12$, $z=30$, $z=50$, $z=67$ and $z=95\text{mm}$ for several times including $t=14\text{days}$, 34d , 76d , 100d , 150d , 200d , 210d , 270d .
- Dry density, water saturation and water content profiles at $R=0\text{mm}$ for several times including $t=14\text{days}$, 34d , 76d , 100d , 150d , 210d , 270d .

References

BEACON, D4.1 report, 2019, Bentonite mechanical evolution – experimental work for the support of model development and validation

BEACON, D5.2 report, 2018, Specifications for Beacon WP5: testing, verification and validation of models. STEP2 – large scale experiments

Hoffmann C., Alonso E.E., Romero E., 2007 - Hydro-mechanical behaviour of bentonite pellet mixtures, *Physics and Chemistry of the Earth* 32 (2007) 832–849

Imbert C, Villar MV, 2006. Hydro-mechanical response of a bentonite pellets/powder mixture upon infiltration. *Applied Clay Science* 32: 197-209.

Lloret, A., Villar, M.V., Sánchez, M., Gens, A., Pintado, X., Alonso, E.E., 2003. Mechanical behaviour of heavily compacted bentonite under high suction changes. *Géotechnique* 53, 27–40. <https://doi.org/10.1680/geot.2003.53.1.27>

Villar, M. V., 2002. Thermo-hydro-mechanical characterisation of a bentonite from Cabo de Grata. PhD thesis, Universidad Complutense, ENRESA Technical Report 04/2002, Madrid.

Villar, M.V. & Lloret, A. 2008. Influence of dry density and water content on the swelling of a compacted bentonite. *Applied Clay Science* 39: 38-49.
DOI: 10.1016/j.clay.2007.04.007